Accepted Manuscript

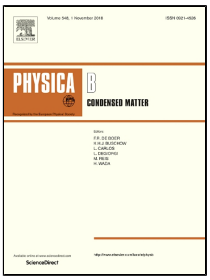

Luminescence and cathodoluminescence properties of $M^{I}Pr(PO_3)_4$ (M^{I}=Na, Li, K) and PrP_5O_{14}

S. Gharouel, L. Labrador-Páez, A. Urbieta, P. Fernández, P. Haro-González, K. Horchani-Naifer, M. Férid

PII:	S0921-4526(18)30739-7
DOI:	10.1016/j.physb.2018.11.037
Reference:	PHYSB 311172
To appear in:	*Physica B: Physics of Condensed Matter*
Received Date:	17 September 2018
Accepted Date:	17 November 2018

Please cite this article as: S. Gharouel, L. Labrador-Páez, A. Urbieta, P. Fernández, P. Haro-González, K. Horchani-Naifer, M. Férid, Luminescence and cathodoluminescence properties of $M^{I}Pr(PO_3)_4$ (M^{I}=Na, Li, K) and PrP_5O_{14}, *Physica B: Physics of Condensed Matter* (2018), doi: 10.1016/j.physb.2018.11.037

Luminescence and cathodoluminescence properties of $M^{I}Pr(PO_3)_4$ (M^{I}=Na, Li, K) and PrP_5O_{14}

By

S. Gharouel[a,*], L. Labrador-Páez[b], A. Urbieta[c], P. Fernández[c], P. Haro-González[b], K. Horchani-Naifer[a], and M. Férid[a]

[a] Laboratoire de Physico-Chimie des Matériaux Minéraux et leurs Applications, Centre National des Recherches en Sciences des Matériaux, B.P.73 Soliman, 8027, Technopole Borj Cedria, Tunisia.

[b] Fluorescence Imaging Group, Departamento de Física de Materiales, Universidad Autónoma de Madrid, C/Francisco Tomás y Valiente, 7, Madrid 28049, Spain.

[c] Departamento Física de Materiales, Fac. Física, Universidad Complutense, Plaza de Ciencias, 1, Ciudad Universitaria, 28040 Madrid, Spain

* E-mail : saidagharouel@gmail.com

ABSTRACT

Poly-crystals of praseodymium phosphate $M^{I}Pr(PO_3)_4$ (M^{I}=Na, Li, K) and PrP_5O_{14} have been synthesized by the flux method. All of these hosts crystallized in the monoclinic structures with different space groups. The spectroscopic properties of trivalent praseodymium ions in these compounds have been characterized. The emission spectra under laser excitation at 488 nm show several characteristic emission bands of Pr^{3+} resulting from intra-configurational transitions between $^3P_0$ and $4f^2$ lower lying levels. All the studied compounds exhibit two strong parity-allowed $4f^15d^1 \rightarrow 4f^2$ emission bands located in the near ultraviolet domain using electrons as source for optical excitation. Therefore, these materials are of interest for applications in lighting and scintillating applications.

Keywords: polyphosphate, ultraphosphate, praseodymium, luminescence, scintillator.

1. INTRODUCTION

Emissions from the $4f^{N-1}5d \rightarrow 4f^{N}$ interconfigurational transitions of trivalent lanthanide ions have received great interest for its potential applications in both ultraviolet (UV) tunable solid-state laser and scintillator devices **[1-3]**. Scintillators are luminescent materials which absorb ionizing radiation, including α-, β-, electron, ion, X- and γ-rays, and emit the absorbed energy in form of UV or visible light. Scintillators, used to detect X- or γ-rays, find several industrial applications including process control, geophysical exploration, container scanning, radiation monitoring, detection of radioactive materials, and medical imaging **[4]**. Cerium compounds are actively investigated because of its good scintillation performance **[5-7]**.

In the last two decades, several works have been devoted to the spectroscopic characteristics of the trivalent praseodymium (Pr^{3+}) ion in diverse inorganic compounds. Indeed, they are promising candidates for applications such as optical thermometry **[8-11]**, luminophors **[12]**, and optical fiber communications **[13-14]**. In addition to their efficient intraconfigurational $4f^2 \rightarrow 4f^2$ transitions, Pr^{3+}-doped materials are well known for exhibiting strong intensity of emission from the electric dipole allowed inter-configurational $4f^15d^1 \rightarrow 4f^2$ transitions, with short decay time, in the order of nanoseconds **[15-17]**. Therefore, Pr^{3+}-doped compounds have received a great interest, owing to their diverse potential applications. In fact, Pr^{3+} hosts that support the $4f^15d^1 \rightarrow 4f^2$ fluorescent emissions can conduct to the development of fast scintillators **[18,19]**, and, in particular, to application in medical diagnostic technics such as positron emission tomographies (PET)**[20,21]**. Moreover, phosphors based on the Pr^{3+} $4f^15d^1 \rightarrow 4f^2$ interconfigurational transition can be employed for some other commercial applications, such as for germicidal purposes **[22]**, detecting alpha and beta particles **[23]**, UV tunable solid state lasers **[24,25]**, and for therapeutical application in medicine **[26]**.

Numerous inorganic materials such as molybdates **[27]**, tungstates **[28]**, aluminates **[29]**, silicates **[30]** and phosphates **[31-33]** are activated by Pr^{3+} ions. Among them, Pr^{3+}-doped

phosphates crystals have been the subject of several investigations in the past years, owing to their excellent characteristics for the development of potential laser applications **[34-36]**, non-contact optical temperature sensing applications **[8]**, and, especially, for fast scintillating materials **[37,38]**. Phosphates exhibit a relatively high stability under standard conditions of temperature and humidity. They also show good crystallinity, they are mechanically rigid, and not soluble in most acids and water. Owing to these interesting characteristics, many works have been devoted to the investigation of spectroscopic properties of Pr^{3+}-doped phosphates, especially concerning ultraphosphates and polyphosphates **[39-43]**. Because of the relatively large distances between rare earth ions in the host, ultraphosphates and polyphosphates are appropriate as hosts for lanthanide ions showing a strong concentration quenching of fluorescence **[44-45]**.

In this work, we report the synthesis by flux method and the characterization of $M^{I}Pr(PO_3)_4$ polyphosphate and PrP_5O_{14} ultraphosphate. The emissions originating from Pr^{3+} 4f-4f and 5d-4f transitions in these crystalline hosts are also studied with the purpose of characterizing them as promising materials for lighting and scintillator technologies.

The comparison of luminescence and scintillation properties of four praseodymium concentrated phosphates $NaPr(PO_3)_4$ ($P2_1/n$), $LiPr(PO_3)_4$ (C2/c), $KPr(PO_3)_4$ ($P2_1$) polyphosphates and PrP_5O_{14} ($P2_1/c$) ultraphosphate was also presented with special emphasis on the influence of the structural differences and monovalent alkali ions on the optical properties.

2. EXPERIMENTAL

2.1. Synthesis method

The $M^{I}Pr(PO_3)_4$ (M^{I}=Na, Li, K) and PrP_5O_{14} poly-crystals were synthesized by using the flux method described in previous works **[46,47]**. A mixture of alkali metal ions carbonates $M^{I}_2CO_3$ and praseodymium oxide (Pr_6O_{11}) were dissolved in phosphoric acid (H_3PO_4 85%) with

appropriate M^I/Pr/P molar ratios. The resulting solution was then thermally treated in a vitreous graphite crucible at temperature between 300-400°C, the heating duration varying between 5 and 7 days. After that, the obtained crystals were washed several times in boiling water in order to remove the excess of phosphoric acid.

2.2. Characterization

The X-ray powder diffraction (XRD) patterns of the obtained compounds have been recorded via X'PERT Pro PANAnalytical diffractometer with Cu-Kα radiation Å (λ= 1.540598 Å) in the range of Bragg angles $10° \leq 2\theta \geq 50°$.

The visible fluorescence spectra have been obtained using a home-made confocal microscope under Ar laser excitation at 488 nm. The decay times have been measured by exciting the $^3P_0$ level of Pr^{3+} ions using a Spectra Physics optical parametric oscillator (MOPO-730) pumped by a Nd:YAG laser (Quanta-Ray CG-230), which delivers pulses of 10 ns duration with a 10 Hz repetition rate.

The cathodoluminescence spectra were recorded by a CCD camera (Hamamatsu PMA-11) attached to a Scanning Electron Microscope (Hitachi S-2500) operated at 15kV.

All these analysis have been made at room temperature.

3. RESULTS AND DISCUSSION

3.1. Structural and size characterization

The registered X-ray diffraction patterns of the prepared samples are shown in Fig.1.

Based on JCPDS, all the samples reveal the absence of phases different from the monoclinic.

The tentative structures of the materials considered in this work are schematized in Fig.2. According to Horchani *et al.* **[48]**, the structure of $NaPr(PO_3)_4$ is characterized by a three-dimensional framework formed by the PrO_8 polyhedron and PO_4 tetrahedron, delimiting tunnels in which the Na^+ ions have been located in the [010] direction (see Fig. 2.a). The

$LiPr(PO_3)_4$ polyphosphate consists of a three-dimensional framework of PrO_8 dodecahedrons, connected by spiral $(PO_3)_n$ infinite chains. The Li^+ cations reside in the tunnels running along the [101] direction delimited by the framework, as mentioned in a previous work for the $LiYb(PO_3)_4$, **[50]** isostructural to $LiPr(PO_3)_4$ (see Fig. 2.b). After literature survey **[51]**, it is concluded that in the crystalline structure of $KPr(PO_3)_4$ the infinite polyphosphate chains are constructed of corner-sharing PO_4 tetrahedrons and the K^+ cations are located at the holes along the *b* direction. These infinite chains are associated by isolated PrO_8 antiprisms to develop the three-dimensional framework (see Fig. 2.c). According to Liu Shu-Zhen *et al*. **[52]**, the structure of the PrP_5O_{14} ultraphosphate is characterized by infinite $(P_5O_{14})^{3-}$ ribbon anions linked through isolated PrO_8 polyhedron (see Fig. 2.d). According to their symmetry properties shown in Fig. 2, it is obvious that all these compounds crystallize in the monoclinic system with different space group. Therefore, it can be noted that the structural characteristics derived from the XRD are in good agreement with those mentioned in the literature.

Comparing the structures of these materials, the presence of many structural differences is noticeable. While in $NaPr(PO_3)_4$ (with space group $P2_1/n$), $LiPr(PO_3)_4$ (with space group C2/c) and PrP_5O_{14} (with space group $P2_1/n$), Pr^{3+} atom occupies 4e crystallographic position **[48,49, 52]**, in $KPr(PO_3)_4$ (with space group $P2_1$), Pr^{3+} atom occupies 2a crystallographic position **[51]**. In addition to the change of the space group of these materials, the comparison of their infrared absorption and Raman scattering spectra, given in a previous work **[8]**, indicate that the non-centrosymmetric structure is only observed for the $KPr(PO_3)_4$ polyphosphate. It is expected that these structural differences be reflected in the spectroscopic properties of Pr^{3+} ions, as their environment changes significantly in the different phosphate hosts, and so it does the crystalline field that the Pr^{3+} ions feel.

Analysis of the size of these materials using scanning electron microscopy and laser granulometry measurements, presented in our previous work **[8]**, proved that the crystals have a size at the microscale.

3.2. Luminescence properties

The luminescence properties of $M^{I}Pr(PO_3)_4$ (M^{I}=Na, Li, K) and PrP_5O_{14} crystalline hosts were evaluated with the aim of assessing their suitability as hosts of the lanthanide ion. Fig. 3.a presents the photoluminescence spectra of the four investigated phosphors in the visible range under excitation at 488 nm. These spectra show visible emission bands that can be attributed to the electronic transitions $^3P_0 \rightarrow {}^3H_J$ (J=5,6) and $^3P_0 \rightarrow {}^3F_J$ (J=2,4) (see Fig. 3.a). The $^3P_0 \rightarrow {}^3H_6$ and $^3P_0 \rightarrow {}^3F_2$ transitions of Pr^{3+} are intense enough to allow a red-orange fluorescence to be observed by the naked eye. Only the fluorescence originated from the $^3P_0$ state is detectable at room temperature, as previously observed in highly concentrated praseodymium phosphors **[32, 34, 36]**. The quenching of the $^1D_2$ luminescence may be explained by the occurrence of non-resonant ($^1D_2$, $^3H_4$) → ($^1G_4$, $^3F_4$) cross relaxation processes, as schematized in Fig. 3.b.

In addition, it is worthy to note that the relative intensity of the band observed around 610 nm and attributed to the $^3P_0 \rightarrow {}^3H_6$ transition remains roughly constant for the various structures and monovalent alkali ions, while the spectral shape of this band is different. In the case of the $NaPr(PO_3)_4$ and $LiPr(PO_3)_4$ polyphosphates, the spectral shape of this band is comparable. In both cases, this band consists of two components separated by a shoulder detected around 611nm, which is most intense in lithium praseodymium polyphosphate. In the case of $KPr(PO_3)_4(P2_1)$, the shoulder, observed at 611nm in $NaPr(PO_3)_4$ and $LiPr(PO_3)_4$, is now a well defined band pointed at 611nm. For the PrP_5O_{14} ultraphosphate, more differences in the intensity of the components of the $^3P_0 \rightarrow {}^3H_6$ emission band are observed. In fact, this band consists of three peaks at 609, 612 and 615nm. The cause of these differences is unambiguous.

Contrary to $KPr(PO_3)_4$ ($P2_1$),the $NaPr(PO_3)_4$($P2_1/n$), $LiPr(PO_3)_4$ (C2/c) and PrP_5O_{14} ($P2_1/c$) hosts have a centrosymmetric structure **[2]**. In opposition to $KPr(PO_3)_4$, in which Pr^{3+} occupies 2a, in $NaPr(PO_3)_4$, $LiPr(PO_3)_4$ and PrP_5O_{14} the trivalent praseodymium ion Pr^{3+} occupies the same symmetry site (4e). Moreover, the monovalent cations occupies, in the $NaPr(PO_3)_4$ and $LiPr(PO_3)_4$ materials, the same symmetric position which is 4e. But, in the potassium praseodymium polyphosphate, K^+ occupies the site 2a. Despite the difference of spectral shape around 610nm, all the samples have the same photoluminescence intensity because the relative intensity of their emission bands is similar.

The decay time of a fluorescent material is an essential parameter for its characterization and potential application in imaging and detection devices **[53]**. Indeed, according to Tyrrell **[54]**, phosphors which present fast decay time with low afterglow, are promising modern pixel detectors intended for fast readout speeds. Moreover, very fast decay phosphors find potential applications in image intensifier tubes for CCD readout devices such as molecular tagging velocimetry, particle imaging velocimetry, and luminescence analysis **[55]**. For these reasons, the decay time of the $^3P_0$ level of Pr^{3+} ion in the analyzed phosphors samples was studied. Very fast exponential $^3P_0$ luminescence decay times were obtained at room temperature for the stoichiometric crystals: 58.9, 61.8, 59.1, and 66.4 ns for $NaPr(PO_3)_4$, $LiPr(PO_3)_4$, $KPr(PO_3)_4$, and PrP_5O_{14}, respectively (Fig.4).

These values are to be compared with the 80 ns measured for the $^3P_0$ decay time in the cyclotetraphosphate $KPrP_4O_{12}$ reported in previous work **[34]**. For this compound, the value of the $^3P_0$ radiative lifetime calculated by M. Malinowski *et al*., using the Jud-Ofelt theory was found to be of the order of 41.6 μs and a fluorescence quenching process relating $^3P_0 \rightarrow {}^1D_2$ multiphonon relaxation was supposed to be the major contribution to the non-radiative decay time.

The very fast exponential $^3P_0$ lifetime observed in $M^IPr(PO_3)_4$ and PrP_5O_{14} may also originate from Pr^{3+}–Pr^{3+} energy transfer processes, since concentrated materials are under consideration. It is to be noticed that the energy transfer between Pr^{3+}ions must be disfavored in all the studied materials owing to the relatively longer value of the distance between its Pr^{3+} ions, of the order of 5.732, 6.488, 6.908, and 5.20 Å for $NaPr(PO_3)_4$, $LiPr(PO_3)_4$, $KPr(PO_3)_4$ and PrP_5O_{14}, respectively, compared with 4.253 Å and in $Pr(PO_3)_3$ and 4.297 Å in $NaPrP_2O_7$ **[38]**. Therefore, the longer the Pr^{3+}–Pr^{3+} distance, the lower the efficiency of the quenching of the $^3P_0$ fluorescence. This fact explains the strong intensities of the observed $^3P_0$ emissions (Fig. 3.a). Because of the relatively large distances between the Pr^{3+} ions, the currently studied phosphates are excellent luminescent hosts, in which the emission of trivalent praseodymium ions is less sensitive to concentration quenching than usual. This property has stimulated the interest on this host and has made stoichiometric praseodymium phosphates commonly used, especially for laser applications **[34-36]**.

3. 3. Cathodoluminescence spectra in the UV range

It is obvious from the precedent results of the photoluminescence characterization that the active ions (Pr^{3+}) in $NaPr(PO_3)_4$, $LiPr(PO_3)_4$, $KPr(PO_3)_4$ and PrP_5O_{14} are efficient luminescent centers. These luminescent properties might origin scintillating processes which is defined as the emission of photons (visible light, UV) produced in a luminescent material when excited by ionizing radiation (α-, β-, electron, ion, X- and γ-rays). On the other hand, the cathodoluminescence is an optical and electromagnetic phenomenon in which electrons impacting on a phosphor, cause the emission of light. Therefore, the cathodoluminescence can be used as an emulator of the scintillation process.

For this reason, we have investigated the cathodoluminescence spectra of studied phosphors. The room temperature cathodoluminesscence spectra of $M^IPr(PO_3)_4$ (M^I=Na, Li, K) and PrP_5O_{14} samples obtained under electron excitation are given in Fig.5. These spectra show two

main intense emission bands at about 250 nm and weaker emission bands at lower energies. These bands can be assigned to parity allowed electric dipole transitions $4f^15d^1 \rightarrow 4f^2$. In addition, it is noticeable that no emission originating from the intra-configurational 4f-4f transition is observed in these spectra. This is probably due to the weakness of the $4f^2 \rightarrow 4f^2$ transitions compared to the observed $4f^15d^1 \rightarrow 4f^2$ ones. Furthermore, it is worthy to note that the relative intensity of the band ascribed to the transitions between the lowest 4f–5d Stark level and the lower lying $4f^2$ states remains approximately constant for the diverse structures and monovalent cations, although the relative intensity of the components varies from sample to sample. In the case of PrP_5O_{14} and $KPr(PO_3)_4$, the spectra are very similar. The most characteristic features are the two intense bands around 250 and 230nm. In both cases, these bands consist of at least two components. In the low energy band a peak at 234nm and a shoulder around 228nm are clearly observed. In the high energy band two clear peaks at 253 and 261nm are clearly observed. For the other two samples more differences are encountered. In the case of $LiPr(PO_3)_4$, these differences affect to the intensity of the components, in particular the shoulder observed at 228nm in PrP_5O_{14} and $KPr(PO_3)_4$, is now a well defined band peaked at 221nm. The high energy band consists of two peaks at 244 and 252nm. The largest differences are found when Na substitutes P. In this case, the highest energy component (app. 220nm) is not visible, and the two main bands are observed between 230-260nm and 305-330nm. The first band consists of three peaks at 232, 250 and 256nm, similar to those observed in the rest of the samples; the second band consists of two well defined peaks at 308 and 328nm. The origin of these differences is not clear. PrP_5O_{14} and $KPr(PO_3)_4$ belong to different symmetry groups and in both compounds the Pr^{3+} occupies different position, the ionic radius of K and P ions is very large (depending on coordination around 1.5 and 0.3Å respectively), the different atomic position could contribute to a better accommodation of the lattice when the large K ions incorporate, hence giving a more relaxed state in which the crystal field perceived

by the Pr^{3+} ions is similar to that in absence of K substitution. In the samples with Li and Na, the atomic position for Pr ions is the same, and the same as in PrP_5O_{14}, however the ionic radii differences (0.6-0.9 Å for Li, and 1-1.4Å for Na) could be responsible for stresses affecting the crystal field and hence the transition probabilities of the different intraionic lines. Further studies would be needed to corroborate this model.

4. CONCLUSION

In the present work, poly-crystals of the $M^IPr(PO_3)_4$ (M^I = Na, Li, K) and PrP_5O_{14} phosphates were synthesized by the flux method and identified using X-ray diffraction. The basic characterization of the spectroscopic properties of Pr^{3+} in $M^IPr(PO_3)_4$ (M^I = Na, Li, K) and PrP_5O_{14} phosphates have revealed that these stoichiometric compounds exhibit intense red–orange emissions corresponding to transitions originating from $^3P_0$ level ($4f^2$-$4f^2$). Furthermore, the decay time of these emissions is of the order of tens of nanoseconds. As a result, $M^IPr(PO_3)_4$ (M^I = Na, Li, K) and PrP_5O_{14} stoichiometric crystals are good candidates for displaying applications.

Furthermore, these Pr^{3+}-doped hosts exhibit intense 5d-4f electric-dipole parity-allowed emission in the UV upon electron excitation. Consequently, these materials have a high potential for their use as scintillators. These concentrated Pr^{3+}-doped compounds, due to their too low mass densities, could be employed in devices intended for detecting high energy particles, such as α, X or γ photons. Finally, it should be noted that the structural differences between ultraphosphates and polyphosphates with chain structure do not seem to play a significant role in the optical and scintillation properties of Pr^{3+} in the analyzed phosphate materials.

5. ACKNOWLEDGMENTS

The authors acknowledge funding support from Carthage University that reports to the Ministry of Higher Education and Scientific Research in Tunisia (99/UR/07-03), Ministerio de Economía y Competitividad de España (MINECO) (MAT2016-75362-C3-1-R and MAT2015-65274-R), the Instituto de Salud Carlos III (PI16/00812), and the Comunidad Autónoma de Madrid (B2017/BMD-3867RENIM-CM). It was co-financed by European Structural and Investment Fund. This work has also been partially supported by COST action CM1403. L.L.-P. thanks the Universidad Autónoma de Madrid for the "Formación de Personal Investigador (FPI-UAM)" program. Dr. Daniel Jaque is gratefully acknowledged for giving us the opportunity to conduct luminescence measurements in the Fluorescence Imaging Group, Department of Material Physics, Madrid Autónoma University.

6. REFERENCES

[1] D.J. Ehrlich, P.F. Moulton, R.M. Osgood Jr., Opt. Lett., 4(1979) 184.

[2] D.J. Ehrlich, P.F. Moulton, R.M. Osgood Jr., Opt. Lett., 5(1980) 339.

[3] P. Dorenbos, R. Visser, C.W.E. van Eijk, N.M. Khaidukov, M.V. Korzhik, IEEE Trans. Nucl. Sci., 40 (1993) 388.

[4] F. De Notaristefani, P. Lecoq, M. Schneegans, , Eds.; Heavy Scintillators for Scientific and Industrial Applications; Editions Frontieres: Gif-sur-Yvette, France, 1993.

[5] C. Dujardin, C. Pedrini, P. Meunier-Beillard, B. Moine, J. C. Gacon, A. Petrosyan, J. Lumin., 72&74 (1997) 759.

[6] W.W. Moses, S.E. Derenzo, A. Fyodorov, M. Korzhik, A. Gektin, B. Minkov and V. Aslanov, IEEE Trans. Nucl. Sci., 42 (1995) 275.

[7] C.L. Melcher, J.S. Schweitzer, Nucl. Instrum. Methods Phys. Res. Sect. A, 314 (1992) 212.

[8] S. Gharouel, L. Labrador-Páez, P. Haro-González, K. Horchani-Naifer, M. Férid, J. Lumin., 201 (2018) 372.

[9] S. Zhou, G. Jiang, X. Wei, C. Duan, Y. Chen, M. Yin, J. Nanosci. Nanotechnol., 14 (2014) 3739.

[10]M.S. Pudovkin, O.A. Morozov, V.V. Pavlov, S.L. Korableva, E.V. Lukinova, Y.N. Osin, V .G. Evtugyn, R.A.Safiullin, V.V. Semashko, J. Nanomater., 2017 (2017)1.

[11] V.K. Rai, S.B. Rai, Appl. Phys. B, 87 (2007)323.

[12] X. Yang, F. Huang, Z. Huang, F. Cao, J. Zhang, RSC Adv., 6 (2016) 65311.

[13] J. Wang, J.R. Hector, D. Brady, D. Hewak, B. Brocklesby, M. Kluth, R. Moore, D.N. Payne, Appl. Phys. Lett., 71 (1997)1753.

[14] D. Machewirth, K. Wei, V. Krasteva, R. Datta, E. Snitzer, G. Sigel J. Non-Cryst. Solids, 213 (1997)295.

[15] C. Dujardin, C. Pedrini, J. Gâcon, A. Petrosyan, A. Belsky, A. Vasilev, J. Phys.: Cond. Matt., 9 (1997) 5229.

[16] M. Laroche, S. Girard, J. Margerie, R. Moncorge, M. Bettinelli, E. Cavalli, J. Phys.: Cond. Matt., 13 (2001) 765.

[17] L. Zhang, C. Pédrini, C. Madej, C. Dujardin, J. C. Gcon, B. Moine, I. Kamenskikh, A. Belsky, D. Shaw, M. Macdonald, P. Mesnard, C. Fouassier, J. C. Van't Spijker, C.W.E. Eijk, Radiat. Eff. Defects Solids, 150 (1999) 47.

[18] P. Dorenbos, M. Marsman, C. Van Eijk, M. Korzhik, B. Mlnkov, Radiat. Eff. Defects Solids, 135 (1995) 325.

[19] C. Van Eijk, P. Dorenbos, R. Visser, IEEE Trans. Nucl. Sci., 41 (1994) 738.

[20] A.M. Srivastava, J. Lumin., 129 (2009) 1419.

[21] C. Ronda, J. Gondek, E. Goirand, T. Jüstel, M. Bettinclli, A. Meijerink, Mater. Res. Soc. Symp. Proc., 1111 (2009) 175.

[22] J.M.A. Caiut, S. Lechevallier, J. Dexpert-Ghys, B. Caillier, Ph. Guillot, J. Lumin., 131 (2011) 628.

[23] Y. Zhou, D.D. Jia, L.A. Lewis, S.P. Feofilov, R.S. Meltzer, Nucl. Instr. Methods Phys. Res.Sect A: Accel. Spectrom. Detect. Assoc. Equip., 633 (2011) 31.

[24] M. Laroche, M. Bettinelli, S. Girard, R. Moncorgé, Chem. Phys. Lett., 311 (1999)167.

[25] S. Nicolas, E. Descroix, M.F. Joubert, Y. Guyot, M. Laroche, R. Moncorgé, R.Y. Abdulsabirov, A.K. Naumov, V.V. Semashko, A.M. Tkachuk, M. Malinowski, Opt. Mater., 22 (2003) 139.

[26] G. Blasse, B.C. Grabmaier, Luminescent Materials, Springer-Verlag, Berlin Heidelberg, 1994.

[27] Q. Li, J. Huang, D. Chen, Eur. Phys. J. Appl. Phys., 51 (2010) 10603.

[28] Y. Huang, T. Tsuboi, H.J. Seo, J. Phys. Chem. A, 112 (2008) 5839.

[29] Y. Fujimoto, O. Ishii, M. Yamazaki, Electron. Lett., 45 (2009)1301.

[30] J.P.M.Van Vliet, G.Blasse, Mater. Res. Bull., 25 (1990) 391.

[31] B. Borkowski, E. Grzesiak, F. Kaczmarek, Z. Kałuski, J. Karolczak, M. Szymański, J. Cryst. Growth, 44 (1978) 320.

[32] Z. Mazurak, E. Lukowiak, B. Jezowska-Trzebiatowska, D. Schultze, Ch. Waligora, J. Phys. Chem. Solids, 45 (1984) 487.

[33] K. Horchani-Naifer, M. Férid, Inorg. Chim. Acta, 362 (2009) 1793.

[34] M. Malinowski, R. Wolski, W. Woliński, J. Lumin., 35 (1986) 1.

[35] C. Szafrański, W. Strek, B. Jezowska-Trzebiatowska, Opt.Commun., 47 (1983) 268.

[36] M. Szymański, J. Karolczak, F. Kaczmarek, Appl.Phys., 19 (1979) 345.

[37] K. Horchani, J.C. Gâcon, C. Dujardin, N. Garnier, M. Ferid, M. Trabelsi-Ayedi, Nucl. Instr. Methods Phys. Res.Sect A: Accel. Spectrom. Detect. Assoc. Equip., 486 (2002) 283.

[38] A. Jouini, J.C. Gacon, M. Ferid, M. Trabelsi-Ayadi, Opt. Mater., 24 (2003) 175.

[39] M-T, Averbuch-Pouchot, A Durif, Topics in phosphate chemistry, Grenoble, 1996.

[40] H. Dornauf, J. Heber, J. Lumin., 22 (1980) 1.

[41] M. Gałczyński, W. Stręk, J. Phys. Chem. Solids, 52 (1991) 681.

[42] Z. Mazurak, E. Łukowiak, B. Jeżowska-Trzebiatowska, Z. Ciunik, D. Schultze, C. Waligora, J. Mol. Struct., 115 (1984) 31.

[43] Y. Bai, Q. Kan, Y. Zhao, T. Li, J. Lumin., 40 (1988) 702.

[44] Z. Mazurak, E. Łukowiak, B. Jeżowska-Trzebiatowska, D. Schultze, C. Waligora, J. Lumin., 31 (1984) 229.

[45] H. Dornauf, J. Heber, J. Lumin., 20 (1979) 271.

[46] G.I. Dorokhova, O.S. Filipenko, L.O. Atovmyan, B.N. Litvin, Russ. J. Inorg. Chem., 33 (1988) 1581.

[47] A. Durif, in: Crystal Chemistry of Condensed Phosphates, Plenum Press, New York, 1995.

[48] K. Horchani-Naifer, J. Amami, M. Férid, J. Rare Earths, 27 (2009) 1.

[49] M.Ferhi, K.Horchani, K.Ben Saad, M.Ferid, Physica B, 407 (2012) 2593.

[50] E. Ben Zarkouna, A. Driss, Acta Crystallogr. E60 (2004) i102.

[51] A. Oudahmane, M. Daoud, B. Tanouti, D. Avignant and D. Zambonb. Acta Cryst., E66 (2010), i59.

[52] L.Shu-Zhen, H.Guang-Yan, H.Ning-Hai, Acta Phys. Sinica, 40 (1991) 64.

[53] J.P. Creasey, G.C. Tyrrell, Rare-Earth-Doped Materials and Devices IV, 3942 (2000) 114.

[54] G.C.Tyrrell, Nucl. Instrum. Methods Phys. Res., Sect. A, 546(2005)180.

[55] P. Hoess, and K. Fleder, Proc. SPIE 4183, 127 (2001) 9.

Figures captions

Fig. 1 X-ray diffraction data of $NaPr(PO_3)_4$ (black), $LiPr(PO_3)_4$ (red), $KPr(PO_3)_4$ (green), and PrP_5O_{14} (blue) and their corresponding JCPDS reference pattern.

Fig.2. The presentation of the structure of $NaPr(PO_3)_4$ – (a); $LiLa(PO_3)_4$ **[49]** isostructural to $LiPr(PO_3)_4$ – (b); $KPr(PO_3)_4$ – (c) ; and PrP_5O_{14} – (d).

Fig.3. Room temperature emission spectra of $NaPr(PO_3)_4$ (black), $LiPr(PO_3)_4$ (red), $KPr(PO_3)_4$ (green), and PrP_5O_{14} (blue), recorded under excitation wavelengths at 488 nm – (a); Energy levels diagram showing excitation, emissions and a possible cross-relaxation mechanism in Pr^{3+} ion – (b).

Fig.4. Fluorescence decay curves of $^3P_0$ level emission under 488 nm laser excitation of $NaPr(PO_3)_4$, $LiPr(PO_3)_4$, $KPr(PO_3)_4$, and PrP_5O_{14}.

Fig.5. Room temperature emission spectra of $NaPr(PO_3)_4$ (black), $LiPr(PO_3)_4$ (red), $KPr(PO_3)_4$ (green), and PrP_5O_{14} (blue) under electron excitation.

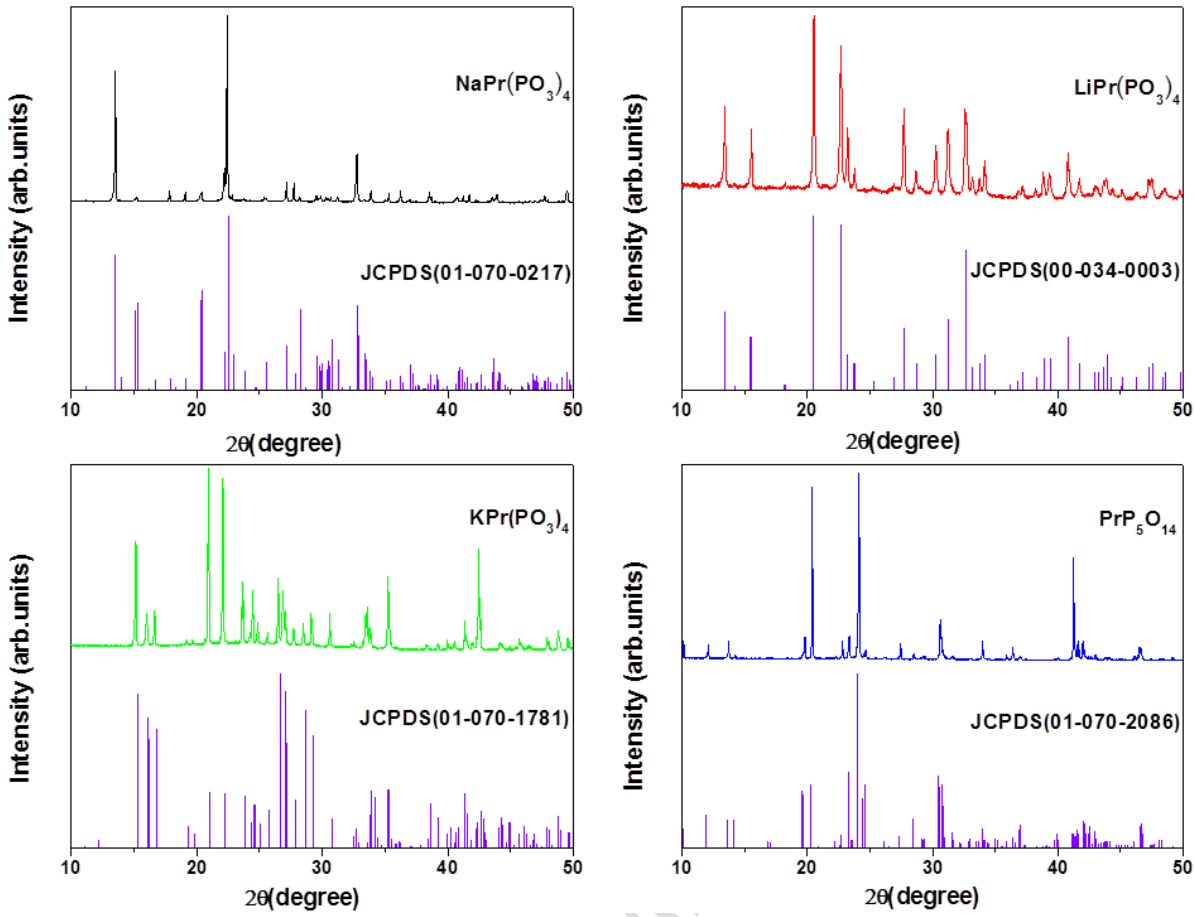

Fig. 1 X-ray diffraction data of $NaPr(PO_3)_4$ (black), $LiPr(PO_3)_4$ (red), $KPr(PO_3)_4$ (green), and PrP_5O_{14} (blue) and their corresponding JCPDS reference pattern.

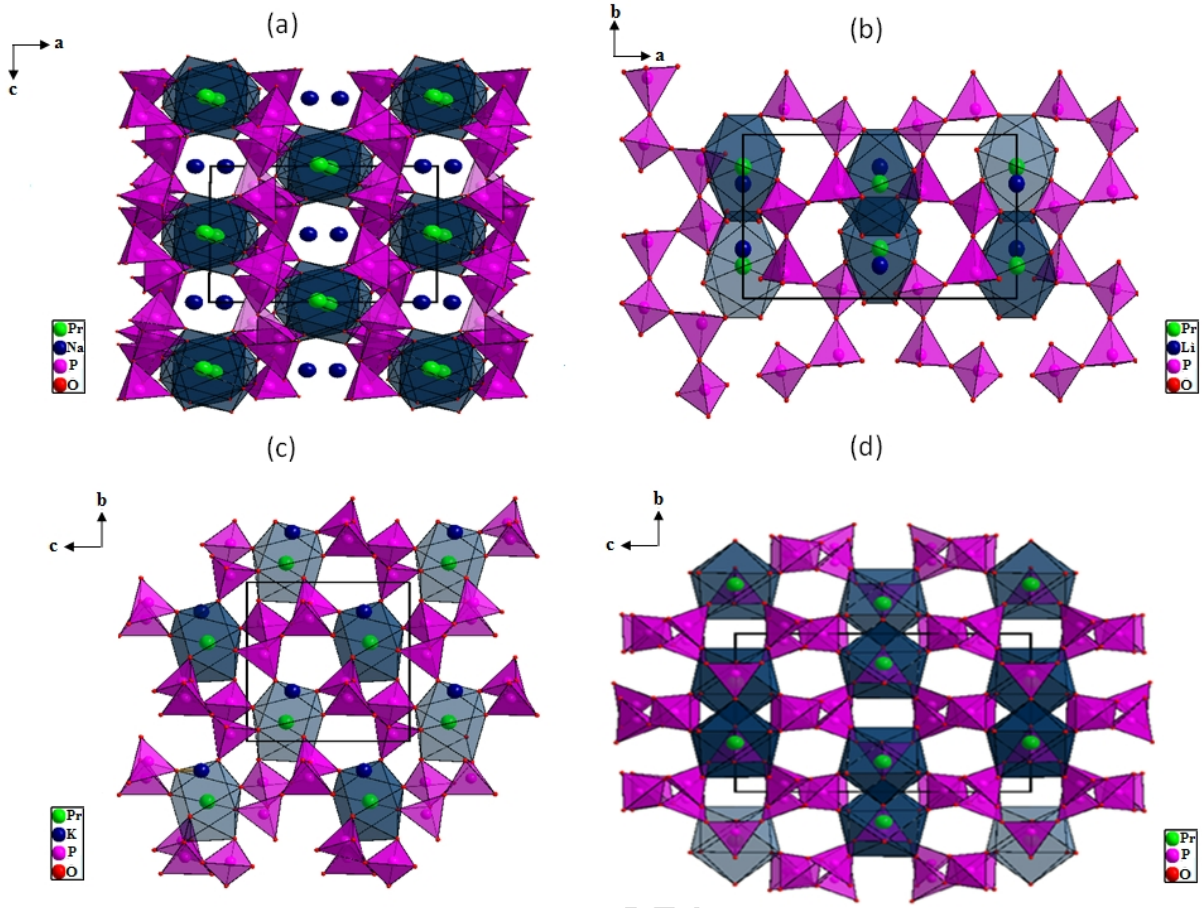

Fig.2. The presentation of the structure of $NaPr(PO_3)_4$ – (a); $LiLa(PO_3)_4$ **[49]** isostructural to $LiPr(PO_3)_4$ – (b); $KPr(PO_3)_4$ – (c) ; and PrP_5O_{14} – (d).

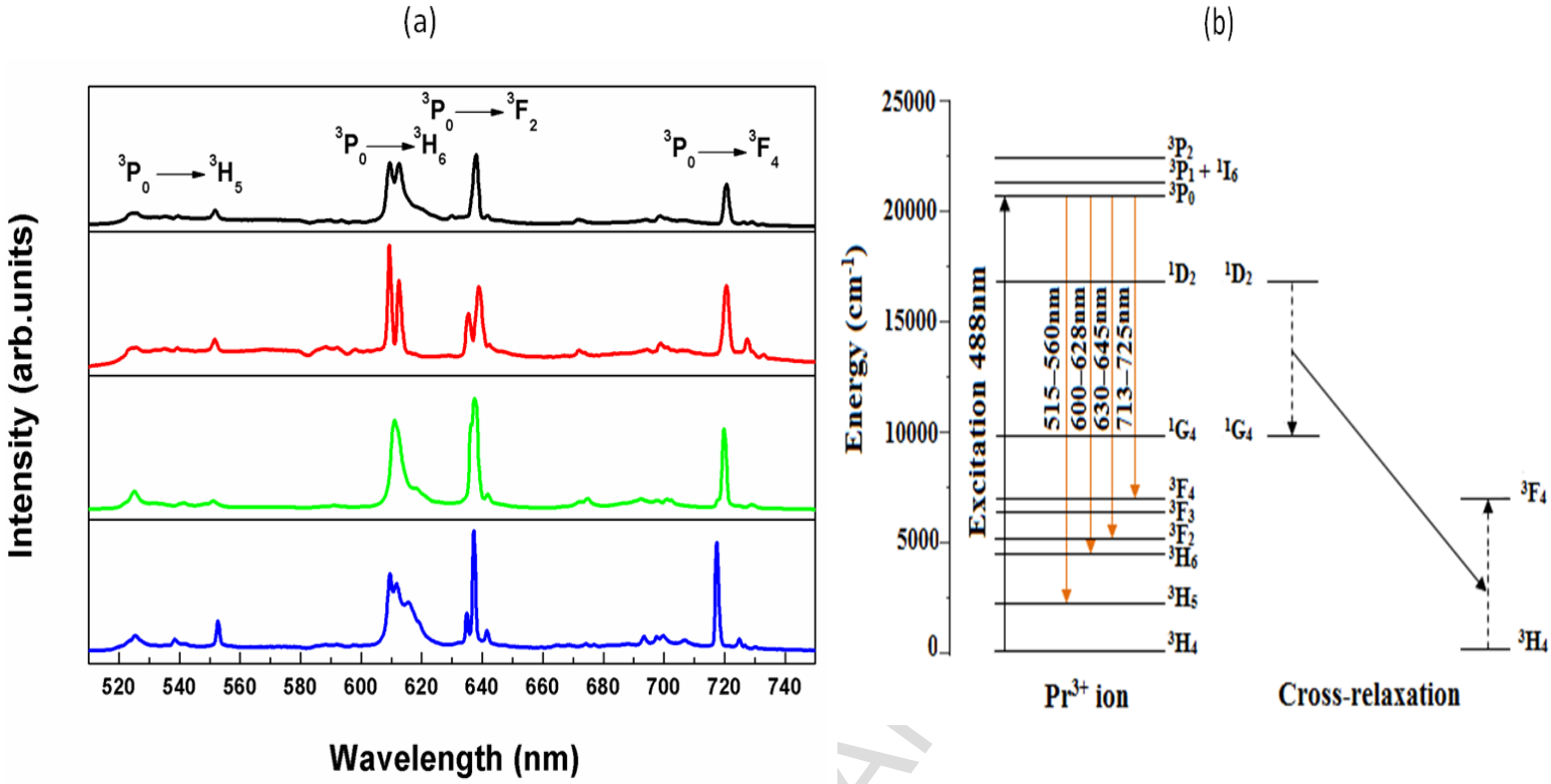

Fig.3. Room temperature emission spectra of $NaPr(PO_3)_4$ (black), $LiPr(PO_3)_4$ (red), $KPr(PO_3)_4$ (green), and PrP_5O_{14} (blue), recorded under excitation wavelengths at 488 nm – (a); Energy levels diagram showing excitation, emissions and a possible cross-relaxation mechanism in Pr^{3+} ion – (b).

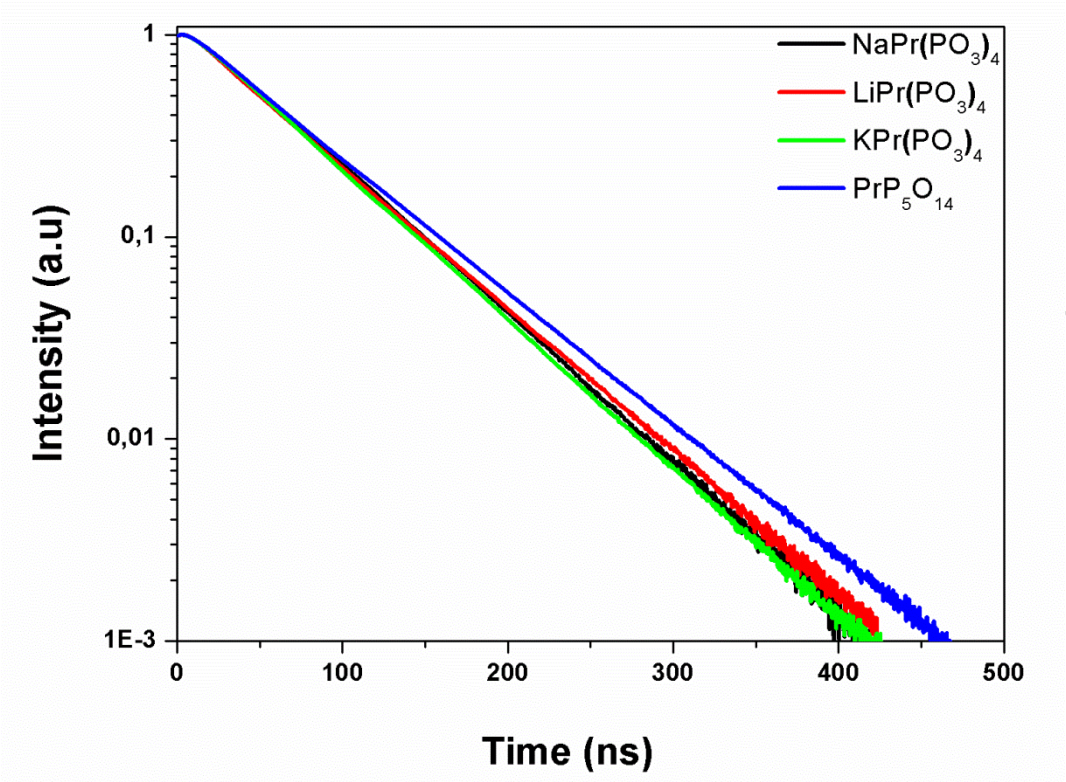

Fig.4. Fluorescence decay curves of $^3P_0$ level emission under 488 nm laser excitation of $NaPr(PO_3)_4$, $LiPr(PO_3)_4$, $KPr(PO_3)_4$, and PrP_5O_{14}.

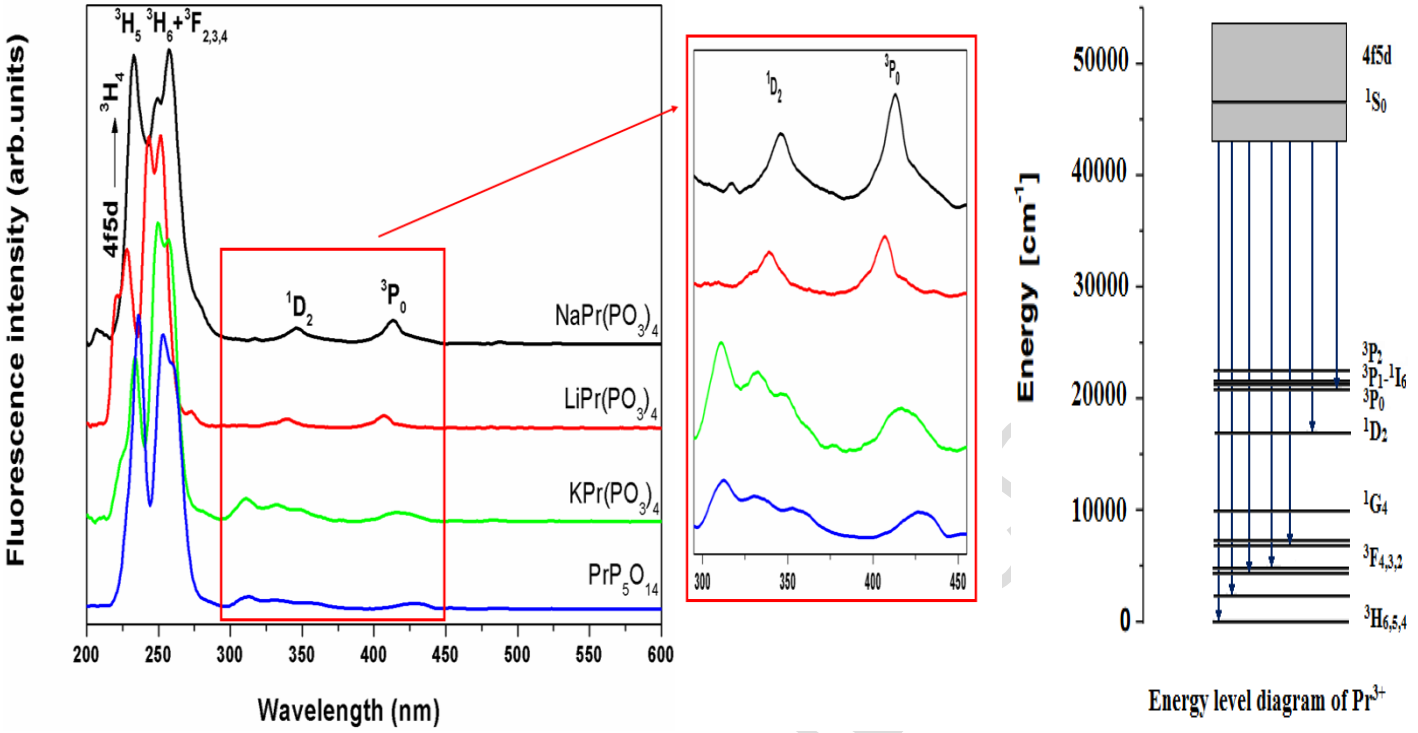

Fig.5. Room temperature emission spectra of $NaPr(PO_3)_4$ (black), $LiPr(PO_3)_4$ (red), $KPr(PO_3)_4$ (green), and PrP_5O_{14} (blue) under electron excitation.